ANTIOXIDANTS & REDOX SIGNALING
Volume 13, Number 12, 2010

DOI: 10.1089/ars.2010.3139

ORIGINAL RESEARCH COMMUNICATION

Redox Stimulation of Cardiomyogenesis *Versus* Inhibition of Vasculogenesis Upon Treatment of Mouse Embryonic Stem Cells with Thalidomide

Nada Milosevic,[1] Mohamed M. Bekhite,[2,*] Fatemeh Sharifpanah,[1,*] Carola Ruhe,[2] Maria Wartenberg,[2] and Heinrich Sauer[1]

Abstract

Thalidomide [α-(*N*-phthalimido)-glutarimide] exerts antiangiogenic properties and causes cardiac malformations in embryos. Herein the effects of thalidomide on cardiovascular differentiation were investigated in mouse embryonic stem (ES) cell-derived embryoid bodies. Thalidomide inhibited the formation of capillary-like blood vessels and decreased tumor-induced angiogenesis in confrontation cultures of embryoid bodies and multicellular prostate tumor spheroids, but stimulated cardiomyogenesis of ES cells. The number of CD31- and CD144-positive endothelial cells was not impaired, suggesting that thalidomide acted on vascular tube formation and cell migration rather than endothelial differentiation. Thalidomide increased reactive oxygen species generation, which was abolished by the NADPH oxidase inhibitor VAS2870 and the complex I respiratory chain inhibitor rotenone. Conversely, thalidomide decreased nitric oxide (NO) generation and endothelial NO synthase activity. VAS2870 abrogated thalidomide stimulation of cardiomyogenesis, whereas inhibition of vasculogenesis persisted. In NOX-1 and NOX-4 shRNA gene-inactivated ES cells, cardiomyogenesis was severely impaired and thalidomide failed to stimulate cardiac cell commitment. The NO donor *S*-nitrosopenicillamine reversed the antiangiogenic effect of thalidomide and increased capillary structure formation, whereas scavenging NO by 2-(4-carboxyphenyl)-4,4,5,5-tetramethylimidazoline-1-oxyl-3-oxide and inhibition of endothelial NO synthase by N^G-nitro-L-arginine methyl ester decreased cardiovascular differentiation. Our data demonstrate that thalidomide causes an imbalance of reactive oxygen species/NO generation, thus stimulating cardiomyogenesis and impairing vascular sprout formation. *Antioxid. Redox Signal.* 13, 1813–1827.

Introduction

THE GLUTAMIC ACID DERIVATIVE thalidomide was developed in the 1950s as potentially an anticonvulsant agent used for the treatment of epilepsy and was later marketed as a sleep aid as well as an antiemetic during pregnancy (31). Ten years later, several reports that described severe malformations in children born to mothers who were treated with thalidomide during pregnancy were published (25, 29). These malformations included phocomelia, defects in long bones, absence of auricles, cleft lip, and cardiac and gastrointestinal anomalies. After >40 years of ban, thalidomide reappeared to the clinical agenda because of its proven clinical activity in erythema nodosum leprosum (47) and—more importantly—for the treatment of multiple myeloma (15). Further, thalidomide proved significant efficiency against a number of different cancers and is currently tested in various anticancer clinical trials (2).

The mechanisms of action of thalidomide have been intensively studied in past years but are still far from being sufficiently unraveled (32). The property of thalidomide to act as an immunomodulator appears to be related to its feature to enhance the mRNA degradation of proinflammatory tumor necrosis factor-α and to inhibit nuclear factor-κB-mediated interleukin-8 expression (43, 49). Further, thalidomide has been shown in several studies to exert antiangiogenic action, presumably through inhibition of vascular endothelial growth factor (VEGF) (22) and fibroblast growth factor-2 (FGF-2) (30) expression and secretion. As proangiogenic growth factors are secreted from tumors to attract blood vessels, it was assumed that thalidomide inhibited tumor growth by interfering with tumor-induced angiogenesis.

[1]Department of Physiology, Justus Liebig University Giessen, Giessen, Germany.
[2]Cardiology Division, Clinic of Internal Medicine I, Friedrich Schiller University Jena, Jena, Germany.
*These authors contributed equally to this work.

Besides inhibiting growth factor secretion, thalidomide was demonstrated by us and others to interfere with angiogenesis through the generation of reactive oxygen species (ROS) (13, 33). This occurs by highly reactive hydroxyl radicals (35), which may exert detrimental effects on endothelial cell differentiation from endothelial progenitor cells as well as on endothelial cell migration and vascular tube formation. Recently, it has been pointed out that thalidomide induces limb defects by preventing angiogenic outgrowth during early limb formation (45).

In the present study, the effects of thalidomide on cardiovascular differentiation of embryonic stem (ES) cells were investigated. This *in vitro* system is excellently suitable for investigations on teratogens that affect the cardiovascular cell lineage because it allows to trace differentiation processes from the emergence of cardiovascular progenitor cells expressing Flk-1 and the primitive streak marker brachyury (17) to terminally differentiated cardiac and vascular cells. It is demonstrated that thalidomide impairs vascular tube formation but not the differentiation of CD31- and CD144-positive endothelial cells. Inhibition of vasculogenesis is counteracted by stimulation of cardiomyogenesis through an imbalance of nitric oxide (NO) *versus* ROS generation.

Materials and Methods

Materials

Thalidomide [*S*(−)-2-(2,6-dioxo-3-piperidinyl)-1*H*-isoindol-1,3(2*H*)-dione] and *N*-(2-mercaptopropionyl)glycine (NMPG) were obtained from Sigma (Deisenhofen, Germany). VAS2870 [3-benzyl-7-(benzoxazolyl) thio-1,2,3-triazolo[4,5-d]pyrimidine] was a gift from Vasopharm (Würzburg, Germany). 2-(4-Carboxyphenyl)-4,4,5,5-tetramethylimidazoline-1-oxyl-3-oxide (carboxy-PTIO), N^G-nitro-L-arginine methyl ester (L-NAME), *S*-nitrosopenicillamine [SNAP; (±)-*S*-nitroso-*N*-acetylpenicillamine], and rotenone were from Calbiochem (Bad Soden, Germany).

Methods

Spinner-culture technique for cultivation of embryoid bodies. To obtain embryoid bodies, ES cells (line CCE) were grown on mitotically inactivated feeder layers of primary murine embryonic fibroblasts in Iscove's medium (Gibco, Live Technologies, Helgerman Court, MD) supplemented with 15% heat-inactivated (56°C, 30 min) fetal calf serum (FCS; Sigma), 2 m*M* glutamine (PAA, Cölbe, Germany), 100 μM 2-mercaptoethanol (Sigma), 1% (v/v) nonessential amino acids stock solution (100×; Biochrom, Berlin, Germany), 1% (v/v) minimal essential medium amino acids (50×; Biochrom), 1 m*M* Na^+-pyruvate (Biochrom), 100 IU/ml penicillin and 100 μg/ml streptomycin (Biochrom), and 1000 U/ml leukemia inhibitory factor (Chemicon International, Hampshire, United Kingdom) in a humidified environment containing 5% CO_2 at 37°C and passaged every 2–3 days. At day 0 of differentiation, adherent cells were enzymatically dissociated using 0.05% trypsin–ethylenediaminetetraacetic acid (EDTA) in phosphate-buffered saline (PBS; Gibco, Helgerman Court, MD) and seeded at a density of 3×10^6 cells/ml in 250-ml siliconized spinner flasks (Integra Biosciences, Fernwald, Germany) containing 125 ml Iscove's medium supplemented with the same additives as described above. Following 24 h, 125 ml medium was added to give a final volume of 250 ml. The spinner flask medium was stirred at 20 rounds per minute using a stirrer system (Integra Biosciences), and 125 ml cell culture medium was exchanged every day. For evaluating the number of beating activity, ~30 embryoid bodies were plated into 6-cm cell culture dishes. Beating activity was evaluated by microscopic inspection. Maximum beating activity of embryoid bodies was observed within 10 days of cell culture. Beating and nonbeating embryoid bodies were determined irrespective of the number of beating foci in individual embryoid bodies.

Culture technique of multicellular spheroids. The human prostate cancer cell line DU-145 was grown routinely in 5% CO_2/humidified air at 37°C with Ham's F10 medium (Gibco) supplemented with 10% FCS (Gibco), 2 m*M* L-glutamine, 0.1 m*M* 2-mercaptoethanol, 1% (v/v) nonessential amino acids (100×), 100 U/ml penicillin, and 50 μg/ml streptomycin. Spheroids were grown from single cells. Cell monolayers were enzymatically dissociated with 0.05% trypsin–EDTA (Gibco), seeded in siliconated 250-ml spinner flasks (Integra Biosciences) with 250 ml complete medium, and agitated at 20 rounds per minute using a Cellspin stirrer system (Integra Biosciences). Cell culture medium was partially (125 ml) changed every day.

Generation of confrontation cultures. Confrontation cultures are tissues generated by culturing three-dimensional tumor spheroids and embryoid bodies in close contact. After few days the tumor spheroid is vascularized by the embryoid body through tumor-induced angiogenesis (48). For the generation of confrontation cultures, multicellular tumor spheroids and embryoid bodies were removed from spinner flasks. To discriminate tumor spheroids grown in confrontation culture from embryoid bodies, tumor spheroids were labeled with the long-term cell tracker dye 5-chloromethylfluorescein diacetate as described previously (11). One embryoid body (4 days old) and one tumor spheroid (10 days old) were inoculated in a 35 μl drop of mixed culture medium (50% spheroid medium, 50% embryoid body medium) placed onto the lid of a 10-cm Petri dish. The lid was turned around and placed on the Petri dish, which was filled with 15 ml of sterile PBS. Within 24 h, embryoid bodies and tumor spheroids closely attached within the hanging drops and were then plated onto Petri-Perm cell culture dishes (Greiner Bio-One, Frickenhausen, Germany).

Immunohistochemistry. As primary antibodies, the rat monoclonal anti-CD31 antibody (Chemicon International) (dilution 1:100), the monoclonal rat-anti-mouse CD31-PE antibody (BD Biosciences, Heidelberg, Germany) (dilution 1:100), the monoclonal rat-anti-mouse CD144 (VE-cadherin) antibody (dilution 1:100), and the monoclonal mouse anti-α-actinin antibody (Sigma) (dilution 1:100) were used. According to the instructions of the manufacturers, the respective tissues were either fixed in ice-cold methanol for 1 h at −20°C and washed with PBS containing 0.01% Triton X-100 (PBST) (Sigma) or were fixed for 20 min at room temperature in 4% formaldehyde in PBS, subsequently washed once in PBS, and fixed for additional 20 min in methanol (−20°C). Blocking against unspecific binding was performed for 60 min with 10% FCS dissolved in 0.01% PBST. For staining, tissues were incubated for 2 h at room temperature with primary antibody (dilution 1:100) dissolved in 0.01% PBST supplemented with 10% FCS. The tissues were thereafter washed three times with

0.01% PBST and reincubated with either a Cy5-conjugated goat anti-rat IgG (H + L) (CD31) or a Cy5-conjugated goat anti-mouse IgG (all from Dianova, Hamburg, Germany) at a 1:200 dilution in 0.01% PBST supplemented with 10% FCS. Control samples were prepared by incubating cells with the isotypic IgG controls and secondary antibodies. Fluorescence recordings were performed using confocal laser scanning microscopy (Leica SP2 AOBS, Bensheim, Germany) with a 5 mW helium/neon laser (single excitation at 633 nm; excitation of Cy5). Emission was recorded at >665 nm. The pinhole settings of the confocal setup were adjusted to give a full width half maximum of 10 μm.

Quantification of vasculogenesis in embryoid bodies. For the quantification of capillary areas within embryoid bodies, an optical sectioning routine based on confocal laser scanning microscopy was used. Images (512×512 pixels) were acquired from CD31-stained embryoid bodies using the extended depth of focus algorithm of the confocal setup. In brief, five full-frame images separated by a distance of 20 μm in *z*-direction were recorded. These images included the information of the capillary area and spatial organization in a tissue slice of 100 μm thickness. From the acquired images, an overlay image giving a three-dimensional projection of the vascular structures in the scanned tissue slice was generated. Using the image analysis facilities of the confocal setup, the branching points of vascular structures within the three-dimensional projection of vascular structures were identified and counted in relation to the size of the respective embryoid body.

Measurement of ROS generation. Intracellular ROS levels were measured using the fluorescent dye 2′,7′-dichlorodihydrofluorescein diacetate (H_2DCF-DA; Molecular Probes, Eugene, OR), which is a nonpolar compound that is converted into a nonfluorescent polar derivative (H_2DCF) by cellular esterases after incorporation into cells. H_2DCF is membrane impermeable and is rapidly oxidized to the highly fluorescent 2′,7′-dichlorofluorescein (DCF) in the presence of intracellular ROS. For the experiments, embryoid bodies were incubated in serum-free medium and treated for times as indicated with different concentrations of thalidomide. Subsequently, 20 μM H_2DCF-DA dissolved in dimethyl sulfoxide was added. After 30 min, intracellular DCF fluorescence (corrected for background fluorescence) was evaluated in 3600 μm^2 regions of interest using an overlay mask. For fluorescence excitation, the 488 nm band of the argon ion laser of a confocal laser scanning microscope (Leica SP2 AOBS) was used. Emission was recorded using an emission band of 515–550 nm. In control microfluorometric experiments, it was excluded that neither thalidomide nor VAS2870 displayed fluorescence properties at the excitation and emission wavelengths used in the present study. We further performed experiments where intracellular ROS were increased by exogenous H_2O_2 (10 and 100 μM) and NO was increased by SNAP (250 n*M*). H_2O_2 robustly increased DCF fluorescence, whereas no fluorescence increase was observed with SNAP, indicating that H_2DCF-DA specifically detected ROS. Neither thalidomide nor VAS2870 affected DCF fluorescence in a cell-free system (data not shown).

Measurement of NO generation. NO generation was evaluated by the use of the cell-permeable specific fluorescent

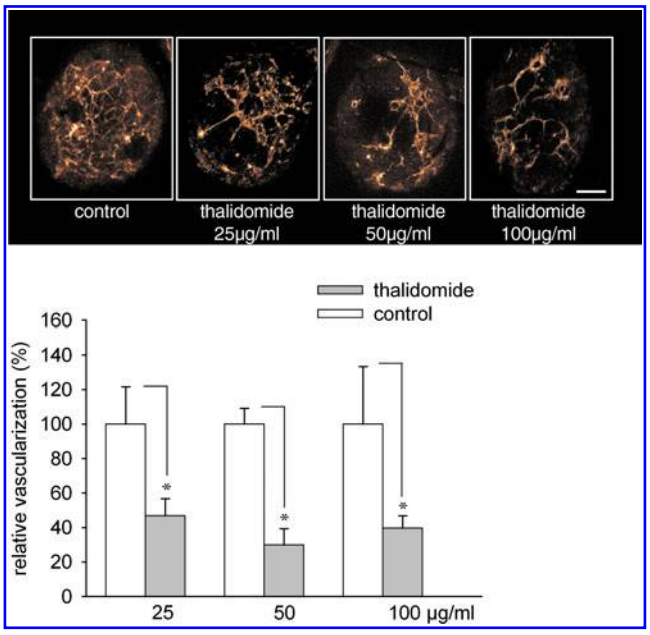

FIG. 1. Effect of thalidomide on vascular differentiation of ES cells. Differentiating embryoid bodies were treated from day 4 to 8 of cell culture with different concentrations of thalidomide and the formation of vascular structures was assessed by semiquantitative CD31 immunohistochemistry. *Upper panel:* Representative embryoid bodies treated with different concentrations of thalidomide ranging from 25 to 100 μg/ml and stained for endothelial structures. From left to right: control, 25 μg/ml thalidomide, 50 μg/ml thalidomide, and 100 μg/ml thalidomide. The bar represents 100 μm. *Lower panel:* Semiquantitative computer-assisted evaluation of vascular branching points upon treatment with different concentrations of thalidomide. *$p < 0.05$, statistically significant when compared with the untreated control. ES, embryonic stem. (For interpretation of the references to color in this figure legend, the reader is referred to the web version of this article at www.liebertonline.com/ars).

NO indicator 4-amino-5-methylamino-2′,7′-difluorofluorescein diacetate (DAF-FM diacetate; Molecular Probes). After incorporation into cells, triazolofluorescein-2 (DAF-2) reacts rapidly with NO in the presence of oxygen to yield the highly fluorescent compound DAF. For NO measurement, 4-day-old embryoid bodies were preincubated with thalidomide for either 4 or 24 h. Embryoid bodies were then incubated for 30 min with 5 μM DAF-FM diacetate dissolved in serum-free medium. After this period, medium was replaced with fresh one and kept for additional 30 min in the incubator to allow complete deesterification of the intracellular diacetate. Subsequently, the embryoid bodies were transferred to an incubation chamber mounted to the inspection table of the confocal setup, and DAF fluorescence was recorded in areas of 3600 μm^2 using the 488 nm argon-ion laser of the confocal setup. Emission was recorded using a longpass LP 515 filter set. In control experiments using H_2O_2 (10 and 100 μM), it was excluded that DAF-FM diacetate detected ROS in the embryoid body system. Neither thalidomide nor VAS2870 affected DAF fluorescence in a cell-free system (data not shown).

Real-time reverse transcriptase–polymerase chain reaction. Total RNA from CCE embryoid bodies treated from day 4 to 8 of cell culture with thalidomide (50 μg/ml) was prepared using Trizol (Invitrogen, Karlsruhe, Germany)

method followed by genomic DNA digestion using DNAse I (Invitrogen). For the analysis of cardiac genes, RNA was isolated on day 8. Total RNA concentration was determined by OD_{260nm} method. cDNA synthesis was performed using 2 μg RNA with MMLV RT (Invitrogen). Primer concentration for quantitative polymerase chain reaction was 150 n*M*. Primer (Invitrogen) sequences are detailed below.

M-HCN4:	forward: 5′-TCCCTCCCTCTTCTTTTT-3′
	reverse: 5′-CTGGTTATTTTCTGCTGTCTT-3′
M-MLC-1a:	forward: 5′-AGAGCTTCGGCATGTCCTTG-3′
	reverse: 5′-TGCTTTACCCAGACATGATGTGC-3′
M-MLC2a:	forward: 5′-GACCCGAGGCAAGGCTG-3′
	reverse: 5′-CTGATTTGCAGATGATCCCAT-3′
M-MLC2v:	forward: 5′-GGCTGACTATGTCCGGGAGA-3′
	reverse: 5′-CTCCGTGGGTAATGATGTGGAC-3′
M-GAPDH:	forward: 5′-GGAGCGAGACCCCACTAACAT-3′
	reverse: 5′-GCGGAGATGATGACCCTTTT-3′

Downregulation of NOX-1 and NOX-4 mRNA using shRNA technique. pLKO.1-puro (Sigma-Aldrich, Taufkirchen, Germany) derivative plasmid carrying shRNA sequence targeting NOX-1 and NOX-4 were separately introduced into CGR8 ES cells by lentiviral particles. Transduced cells with pLKO.1 vector (containing nonhairpin insert) were used as negative control. Lentiviral particles were generated using Human Embryonic kidney 293FT-based amphotropic Phoenix pack-

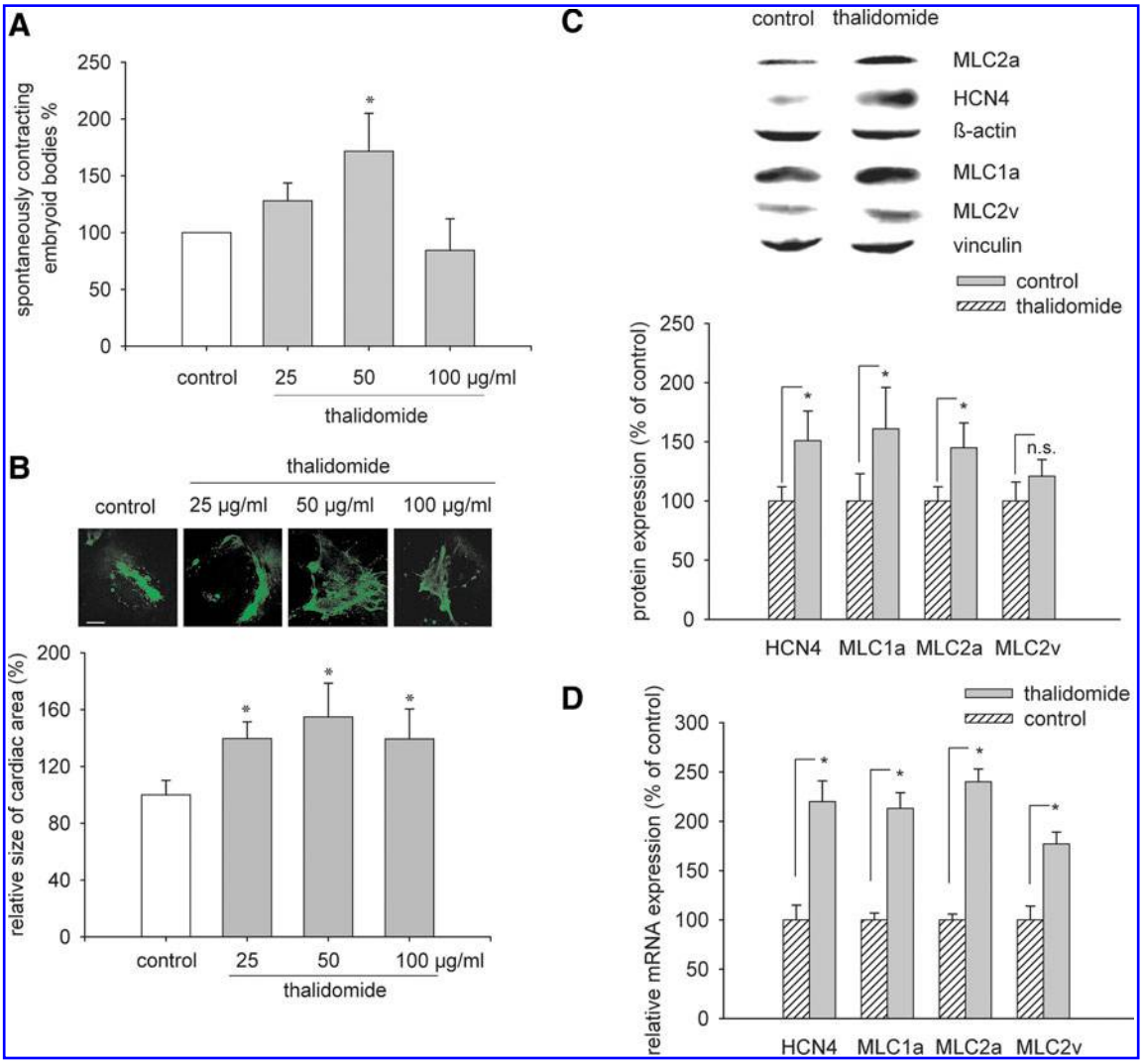

FIG. 2. Stimulation of cardiomyogenesis by thalidomide. Four-day-old embryoid bodies were treated until day 10 of differentiation with thalidomide in concentrations ranging from 25 to 100 μg/ml. On day 4 of differentiation, embryoid bodies were plated onto Petri-Perm dishes and the percentage of spontaneously contracting embryoid bodies (**A**) as well as the size of the contracting areas after immunostaining against α-actinin were assessed. The *upper panel* in **B** shows representative embryoid bodies after α-actinin staining, demonstrating that thalidomide increased beating areas. The bar represents 100 μm. The *lower panel* in **B** shows a quantitative computer-assisted analysis of the cardiac areas in different preparations. (**C**) Western blot and (**D**) mRNA (real-time reverse transcriptase–polymerase chain reaction) expression analysis of markers specific for cardiac cell subtypes, that is, MLC2a and MLC1a for atrial cells, HCN4 for pacemaker cells, and MLC2v for ventricular cells. β-actin and vinculin were used as loading controls. Quantitative analysis of gray level values are shown in the respective lower panels. *$p < 0.05$, statistically significant when compared with the untreated control. (For interpretation of the references to color in this figure legend, the reader is referred to the web version of this article at www.liebertonline.com/ars).

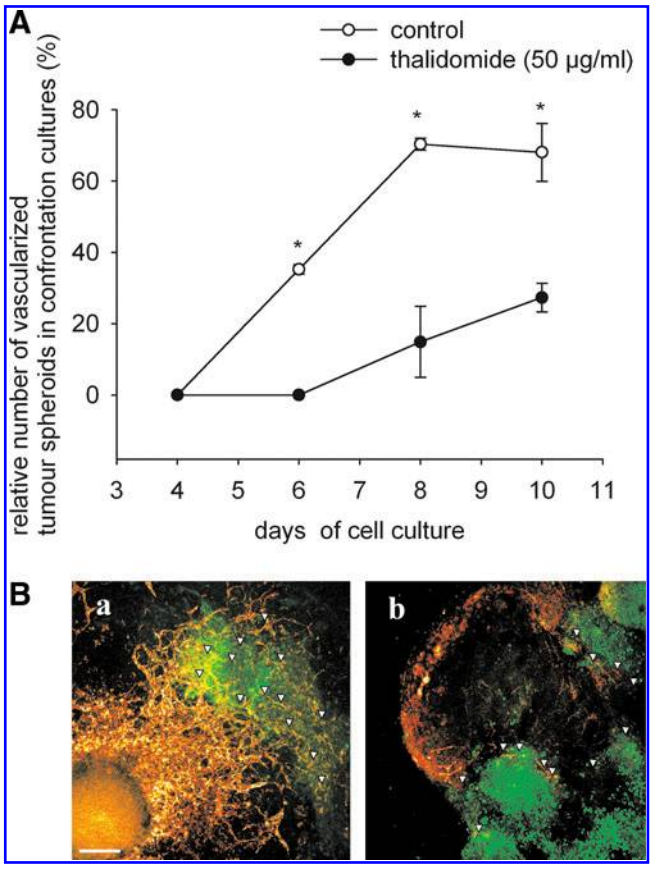

FIG. 3. Inhibition of tumor-induced angiogenesis by thalidomide. (**A**) The time course of tumor-induced angiogenesis in confrontation cultures consisting of embryoid bodies and multicellular DU-145 prostate tumor spheroids, which either remained untreated or were treated with 50 μg/ml thalidomide. (**B**) Representative confrontation cultures are shown. (**a**) Untreated control; (**b**) thalidomide-treated confrontation culture. Confrontation cultures were treated from day 4 to 8 with 50 μg/ml thalidomide. The tumor tissue was stained with the long-term cell tracker dye 5-chloromethylfluorescein diacetate (green) to discriminate between the embryoid body and the tumor tissue. Cells positive for the endothelial cell marker CD31 are presented in red (glow scale). The bar represents 100 μm. The arrow heads indicate sites of vascular sprouting. *$p < 0.05$, statistically significant when compared with the untreated control. (For interpretation of the references to color in this figure legend, the reader is referred to the web version of this article at www.liebertonline.com/ars).

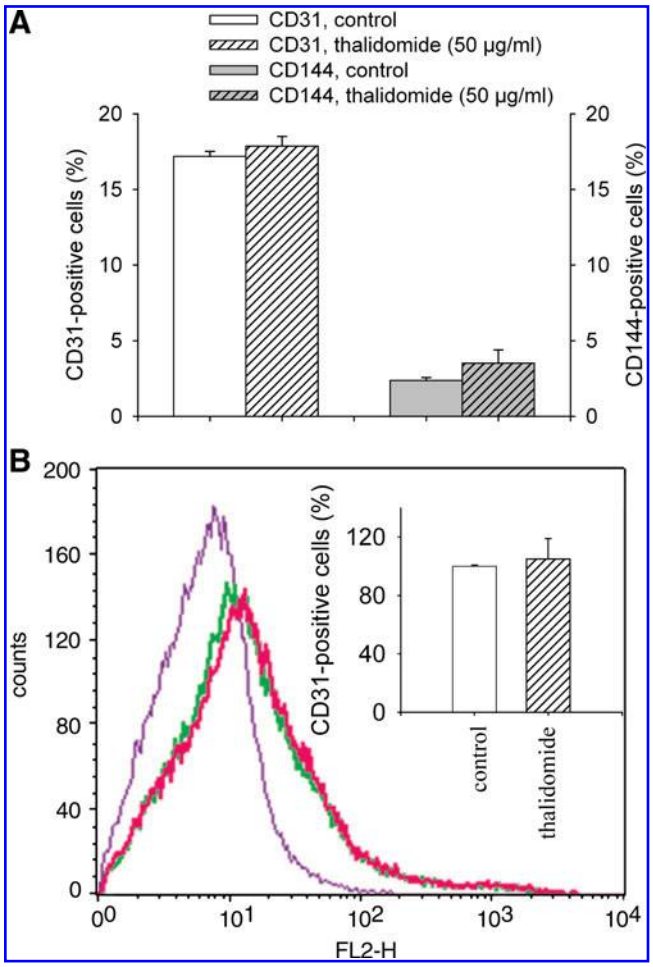

FIG. 4. Thalidomide does not inhibit endothelial cell numbers. Effect of thalidomide on the numbers of either CD31- or CD144-positive endothelial cells in (**A**) embryoid bodies and (**B**) confrontation cultures of embryoid bodies and DU-145 prostate tumor spheroids. Cell numbers were assessed following enzymatic dissociation of either embryoid bodies or confrontation cultures, and cells either positive for CD31 or CD144 were determined by fluorescence-activated cell sorting analysis. Note that thalidomide (50 μg/ml) did not decrease the percentage of cells expressing endothelial cell markers, suggesting that thalidomide is inhibiting vascular sprouting and tube formation. The blue line in **B** represents the isotypic IgG control; the green line, the untreated control; and the red line, the thalidomide-treated sample. The inset in **B** represents the percentage of CD31-positive cells in relation to the untreated control, which was set to 100%. (For interpretation of the references to color in this figure legend, the reader is referred to the web version of this article at www.liebertonline.com/ars).

aging cells (Phoenix-Ampho; Invitrogen) cultured in Dulbecco's Modified Eagle Medium supplemented with 10% FCS and 1% sodium pyruvate plus penicillin/streptomycin. For a 10-cm dish, lentiviral vector plasmids (10 μg) were cotransfected with plasmids encoding the HIV-Rev (5 μg), HIV-MDL (10 μg), and the ecotropic envelope (2 μg) in the presence of polyethylenimine (70 μg; Sigma-Aldrich). Supernatants were harvested after 24 and 48 h and filtrated through 0.22-mm filters. Supernatants were added to CGR8 cells, which were plated in a well of a six-well plate, centrifuged at 400 *g* in a cell culture centrifuge for 1 h, and replaced with fresh medium on the following day. A total of three infection rounds were carried out within 48 h. At the following day the cells were passaged and selected with 2 μg/ml puromycin (Sigma-Aldrich) for 10–14 days. Transduction effectiveness was assessed *via* GFP™ control vector (Sigma-Aldrich). Downregulation was analyzed by Western blot and found to be ~50% (data not shown).

Western blot assay. The western blot assays were carried out after washing the embryoid bodies in PBS and lysing in lysis buffer (20 m*M* Tris-HCl [pH 7.5], 150 m*M* NaCl, 1 m*M* EDTA, 1 m*M* ethylene glycol tetraacetic acid, 1% Triton X-100, 2.5 m*M* sodium pyrophosphate, 1 m*M* β-glycerophosphate, and

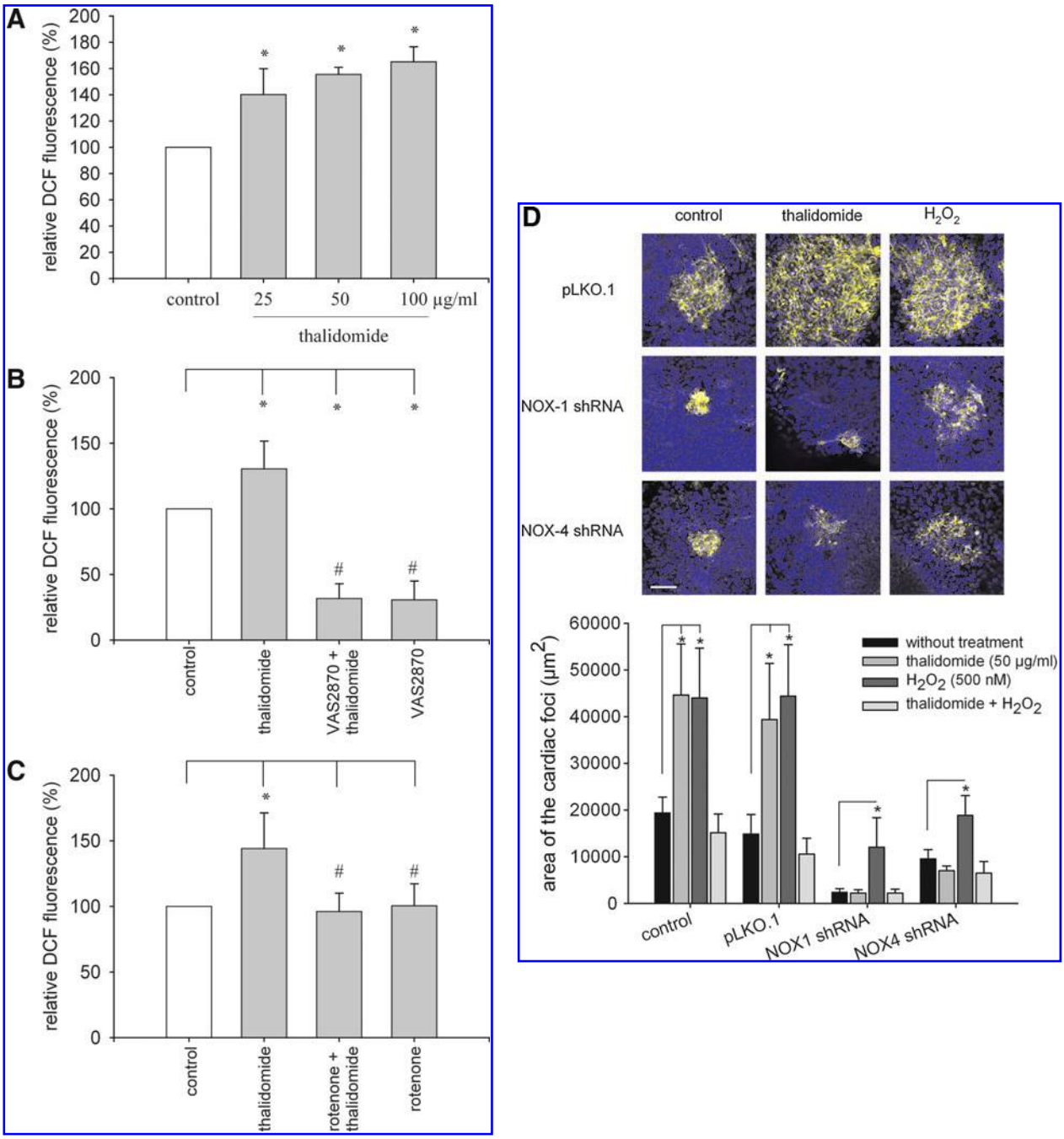

FIG. 5. ROS generation by thalidomide, sources of thalidomide-induced ROS, and impact of NOX-1 and NOX-4 for the thalidomide-induced stimulation of cardiomyogenesis. (**A**) Increase in ROS generation in embryoid bodies upon treatment with different concentrations of thalidomide ranging from 25 to 100 μg/ml. Four-day-old embryoid bodies were treated for 4 h with thalidomide and subsequently stained with 20 μM of 2′7′-dichlorodihydrofluorescein diacetate. ROS generation was evaluated as DCF fluorescence. Note that thalidomide dose-dependently increased ROS generation. (**B**) Effects of the NADPH oxidase inhibitor VAS2870 on thalidomide-induced ROS generation. (**C**) Effects of the respiratory chain complex I inhibitor rotenone on thalidomide-induced ROS generation. (**D**) Effects of shRNA gene inactivation of NOX-1 and NOX-4 on the formation of α-actinin-positive cardiac cell areas. *Upper panel:* Representative images of α-actinin-positive cardiac cell areas (yellow) in embryoid bodies cultivated from ES cells transfected with empty vector (pLKO.1) or NOX-1 and NOX-4 shRNA gene-inactivated ES cells. Cell nuclei of all cells were labeled by Sytox green (blue). Embryoid bodies were cultivated in either the absence (control) or presence of 50 μg/ml thalidomide. As a positive control, embryoid bodies were treated with 500 n*M* H_2O_2. The bar represents 100 μm. The *lower panel* shows a quantitative evaluation of cardiac areas under experimental conditions as indicated. Note that thalidomide failed to increase cardiac areas in NOX-1 and NOX-4 gene-inactivated embryoid bodies, whereas a partial rescue could be achieved by exogenous addition of H_2O_2. Rescue of cardiomyogenesis was not observed upon coadministration of thalidomide with H_2O_2. $^{*,\#}p < 0.05$, statistically significant as indicated. ROS, reactive oxygen species; DCF, 2′,7′-dichlorofluorescein. (For interpretation of the references to color in this figure legend, the reader is referred to the web version of this article at www.liebertonline.com/ars).

1 m*M* Na_3VO_4) that contained 1 m*M* phenylmethylsulfonyl fluoride (a protease inhibitor) for 30 min on ice. Samples were centrifuged at 13,000 *g* for 10 min to pellet the debris. After determination of the protein concentration using a Bio-Rad protein assay (Bio-Rad, Munich, Germany), 20 μg of protein samples was boiled, separated in 12% sodium dodecyl sulfate–polyacrylamide gels, and transferred to nitrocellulose membranes by electroblotting at 80 V for 3 h. Membranes were blocked with 5% (wt/vol) dry fat-free milk powder in Tris-buffered saline with 0.1% Tween for 60 min at room temperature. Incubation with primary antibodies was performed at 4°C overnight. Primary antibodies used were monoclonal mouse anti-HCN4, -MLC1a (Abcam, Cambridge, United Kingdom), -MLC2a, -MLC2v (Synaptic Systems, Göttingen, Germany), -vinculin (Sigma), -β-actin (Cell Signaling, Boston, MA), and -endothelial NO synthase (eNOS) (BD Biosciences) and polyclonal rabbit anti-p-Ser1177 eNOS (Cell Signaling). After washing with Tris-buffered saline with 0.1% Tween, the membrane was incubated with a horseradish peroxidase-conjugated secondary antibody (Cell Signaling Technology, Frankfurt, Germany) for 60 min at room temperature. The blot was developed using the ECL detection kit (Amersham, Freiburg, Germany) to produce a chemiluminescence signal.

Flow cytometry. Embryoid bodies (day 8) were separated into single-cell suspension by incubation for 15 min in collagenase B solution (1.0 mg/ml; Roche Diagnostics, Mannheim, Germany). Cells (1×10^6) were counted and blocked against unspecific binding using 10% FCS in PBS for 15 min on ice. Staining was performed using the direct conjugated antibody CD31-PE (3 μg) (BD Biosciences) or the appropriate PE-rat IgG (Biozol Diagnostica, Munich, Germany) isotype control. Further, the unconjugated monoclonal rat anti-mouse CD144 (VE-cadherin) or the isotype control rat PE-Cy5 was used. For the analysis of CD144, cells were washed and incubated with goat-anti-rat IgG PE-Cy5 (Santa Cruz Biotechnology, Santa Cruz, CA). After three times washing with PBS, cells were analyzed by flow cytometry (FACS Calibur; BD Biosciences) using an argon laser (488 nm) as excitation source and a detector channel at 670 nm.

Statistics

In each experiment, at least 30 embryoid bodies or confrontation cultures were analyzed. Either one-way analysis of variance or Student's *t*-test for unpaired data was applied as appropriate. A *p*-value of <0.05 was considered significant.

Results

Effects of thalidomide on cardiovascular differentiation of ES cells

Recently, the teratogenicity of thalidomide was ascribed to its effects to act as an antiangiogenic agent that induces limb defects by preventing angiogenic outgrowth during early limb formation (45). Previously, we had shown that thalidomide inhibited capillary-like structure formation in ES cell-derived embryoid bodies, which could be attributed to the generation of hydroxyl radicals by this compound (35). In the present study, we investigated the effects of thalidomide on cardiac and vascular differentiation to obtain deepened insights into the mechanisms of thalidomide action. It was ap-

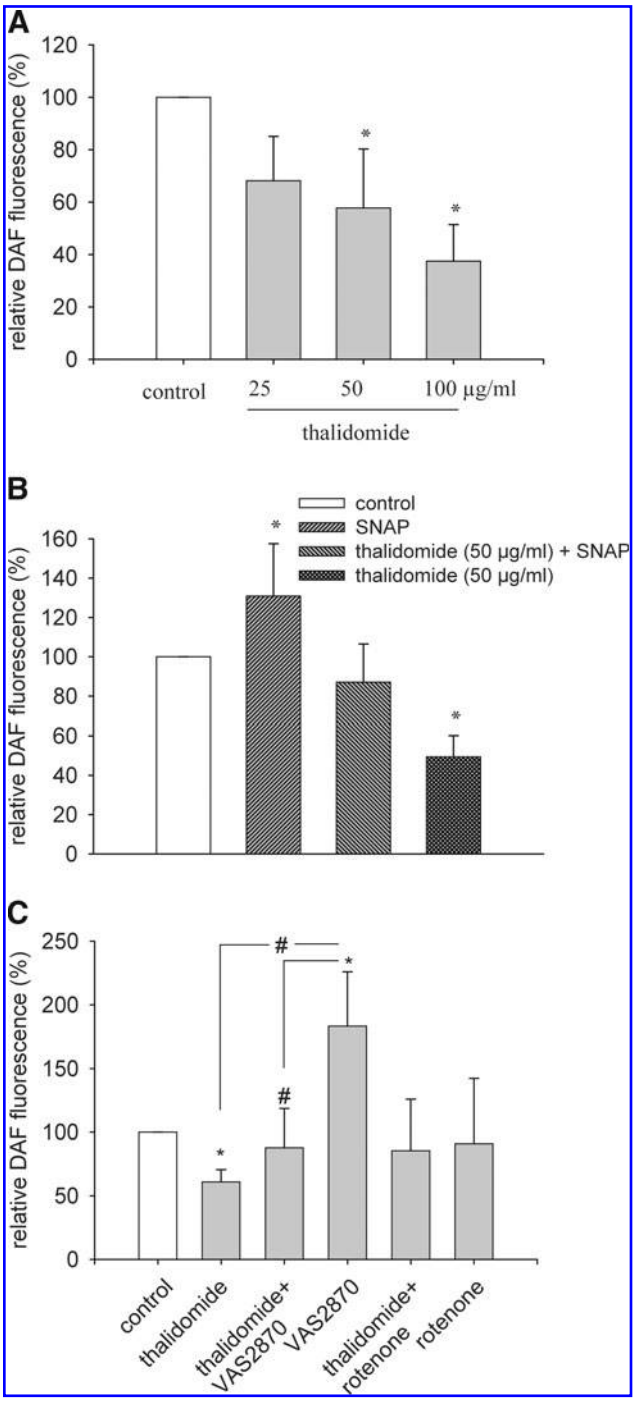

FIG. 6. Inhibition of NO generation by thalidomide and effects of the NO donor SNAP. (**A**) Four-day-old embryoid bodies were incubated with different concentrations of thalidomide ranging from 25 to 100 μg/ml and NO generation was evaluated after 4 h by DAF fluorescence. (**B**) Embryoid bodies were treated with the NO donor SNAP (250 n*M*), with thalidomide (50 μg/ml) alone, or with a combination of SNAP and thalidomide. It was evident that SNAP elevated NO generation and reversed the inhibition of NO generation under thalidomide treatment. (**C**) Effect of the NADPH oxidase inhibitor VAS2870 (50 μM) and the respiratory chain complex I inhibitor rotenone (10 μM) on NO generation. $^{*,\#}p < 0.05$, statistically significant when compared with the untreated control. SNAP, *S*-nitrosopenicillamine; DAF, triazolofluorescein; NO, nitric oxide.

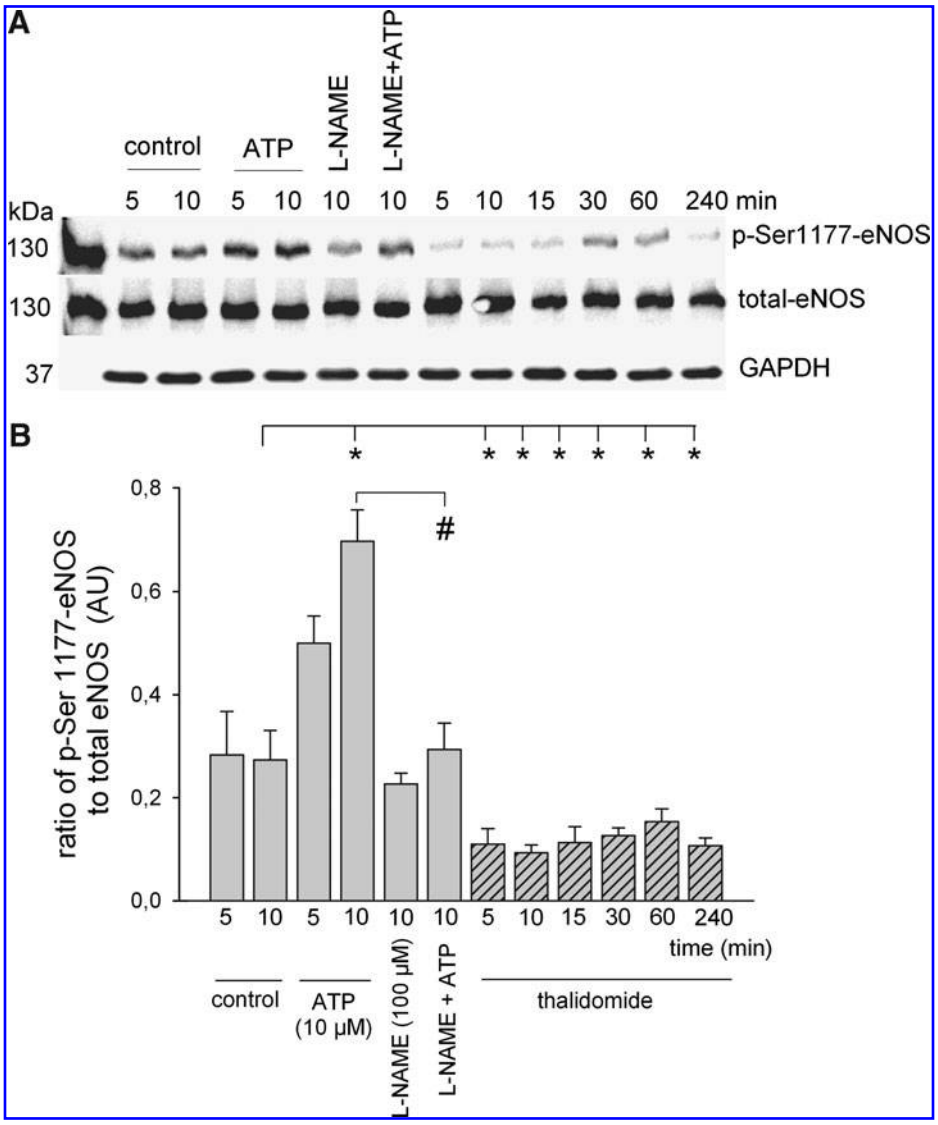

FIG. 7. Inhibition of eNOS phosphorylation by thalidomide. Five-day-old embryoid bodies were incubated for different times as indicated with 50 μg/ml thalidomide and the phosphorylation of eNOS as well as protein expression of nonphosphorylated (total) eNOS was assessed using Western blot analysis. As a positive control, embryoid bodies were treated with 10 μM ATP, which is known to activate eNOS. L-NAME was used as an inhibitor of NOS. *Upper panel:* Representative Western blot of $n = 3$ experiments showing p-Ser1177-eNOS phosphorylation, expression of total nonphosphorylated eNOS, and GAPDH as loading control. Embryoid bodies remained untreated (control), were treated with ATP, or were treated with thalidomide (50 μg/ml) and fixed after 5, 10, 15, 30, 60, and 240 min. *Lower panel:* Quantitative analysis of Western blot gray level values after different times of incubation with thalidomide as indicated. Note that thalidomide significantly downregulated eNOS phosphorylation after 5 min of incubation. $^{*,\#}p < 0.05$, statistically significant as indicated. eNOS, endothelial NO synthase; L-NAME, N^G-nitro-L-arginine methyl ester; GAPDH, glyceraldehyde 3-phosphate dehydrogenase.

parent that thalidomide dose-dependently inhibited vascular sprout formation in embryoid bodies in a concentration range of 25–100 μg/ml (Fig. 1, $n = 4$). In contrast to the inhibition of vascular sprout formation, a significant stimulation of cardiomyogenesis was observed as evaluated by counting the number of spontaneously contracting embryoid bodies (Fig. 2A, $n = 4$) and evaluating the cardiac cell area staining positive for α-actinin (Fig. 2B, $n = 4$). Further, thalidomide increased protein (Fig. 2C, $n = 3$) and mRNA (Fig. 2D, $n = 3$) expression of markers specific for cardiac cell subtypes, that is, MLC2a and MLC1a for atrial cells, and HCN4 for pacemaker cells and MLC2v for ventricular cells as evaluated by western blot technique and real-time reverse transcriptase–polymerase chain reaction, respectively.

Thalidomide inhibits tumor-induced angiogenesis in confrontation cultures of embryoid bodies and multicellular prostate cancer spheroids

As the potential of thalidomide to act as an antiangiogenic agent that owns the capacity to inhibit tumor-induced angiogenesis has been evaluated in several clinical trials (2), tumor vascularization of DU-145 prostate tumor spheroids was investigated in confrontation cultures with vascularized embryoid bodies. It was evident that thalidomide significantly reduced the time course of tumor vascularization and the number of vascularized tumor spheroids when compared with the untreated controls (Fig. 3A, $n = 3$). Further, the number of branching points in vascularized tumor spheroids was significantly reduced in the presence of thalidomide (Fig. 3B, $n = 3$), which clearly underscores the meaning of this compound as an anticancer agent.

Thalidomide reduces vascular sprout formation but not the differentiation of CD31- and CD144-positive endothelial cells

Thalidomide may inhibit vasculogenesis by antagonizing the differentiation of ES cells toward endothelial cells or, alternatively, may affect vascular tube formation from preexisting endothelial cells. To address this issue, fluorescence-activated cell sorting analysis was performed after enzymatic dissociation of 8-day-old embryoid bodies that were treated from day 4 to 8 with 50 μg/ml thalidomide. Subsequently,

the numbers of cells positive for either CD31 or CD144 (VE-cadherin) were analyzed. It was apparent that upon incubation with thalidomide the cell number of $CD31^+$ ($n = 5$) and $CD144^+$ ($n = 10$) cells was not significantly changed (Fig. 4A), which indicates that thalidomide interfered with vascular sprout formation rather than endothelial cell differentiation from ES cells. Consequently, no significant change in the number of CD31-positive cells was observed in confrontation cultures treated with thalidomide (Fig. 4B, $n = 3$).

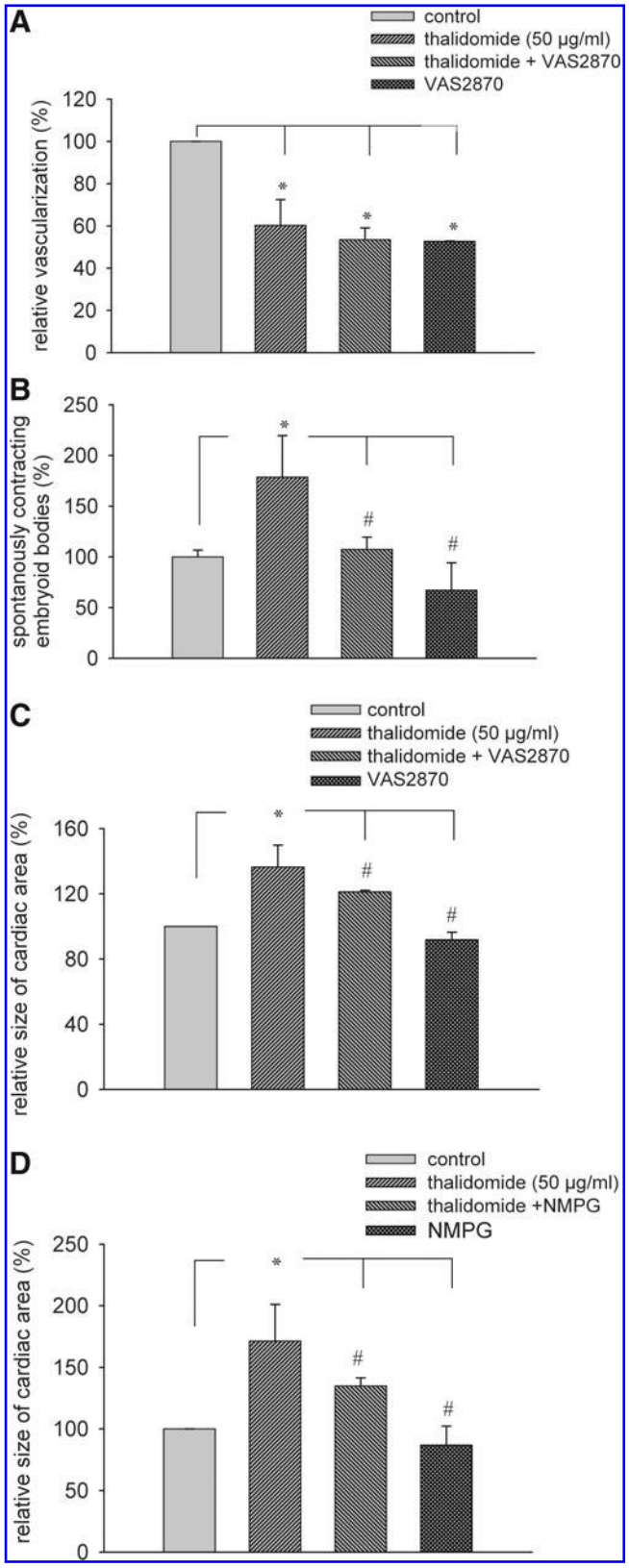

Stimulation of ROS generation in embryoid bodies

ROS may act as signaling molecules that stimulate cardiovascular differentiation of ES cells (3, 5, 34). However, high concentrations of ROS may also exert cytotoxic activities, particularly if highly reactive hydroxyl radicals are formed. As previously shown (35), thalidomide dose-dependently increased ROS generation in embryoid bodies following either 4 or 24 h (data not shown) of exposure toward the compound (Fig. 5A, $n = 4$). This enhanced ROS generation was not due to an increase of NADPH oxidase expression because neither the NOX-1, NOX-2, nor NOX-4 isoform was upregulated upon thalidomide treatment as evaluated by semiquantitative immunohistochemistry (data not shown). Coadministration of the specific NADPH oxidase inhibitor VAS2870 (50 μM) depressed ROS generation below the level of the untreated control. Likewise, a significant inhibition of endogenous ROS generation was achieved with VAS2870 (Fig. 5B, $n = 4$), which clearly indicates that thalidomide-induced as well as endogenous ROS generation are mediated through NADPH oxidase. To further specify the role of NOX isoforms in cardiomyogenesis, shRNA gene inactivation for NOX-1 and NOX-4 was performed (Fig. 5D, $n = 3$). Apparently, thalidomide as well as exogenous addition of H_2O_2 (500 n*M*) significantly increased α-actinin-positive cell areas in control cells and ES cells transfected with empty vector (pLKO.1). In contrast, cardiac area formation was severely impaired in shRNA NOX-1 and NOX-4 ES cells. In the latter, thalidomide failed to stimulate cardiomyogenesis. However, a partial rescue could be achieved by exogenous addition of H_2O_2. This partial rescue was absent when thalidomide was coadministered with H_2O_2. Further, rotenone (2.5 μM), an inhibitor of complex I of the mitochondrial respiratory chain, abolished the increase in thalidomide-induced ROS generation, whereas no effect of this substance was observed when ROS generation was assessed in the absence of thalidomide (Fig. 5C, $n = 3$). From these experiments it was concluded that thalidomide

FIG. 8. ROS inhibition blunts thalidomide-induced cardiomyogenesis but does not reverse vasculogenesis. Effects of ROS inhibition on thalidomide-induced inhibition of vasculogenesis (**A**) and on thalidomide-mediated stimulation of cardiomyogenesis (**B**–**D**). Four-day-old embryoid bodies were treated from day 4 to 10 with 50 μg/ml thalidomide in the absence or presence of 50 μM VAS2870 (**A**–**C**) or with 100 μM of the free radical scavenger *N*-(2-mercaptopropionyl)glycine. Vascularization was assessed by determination of CD31-positive branching points (see **A**). Cardiomyogenesis was investigated by determination of the percentage of spontaneously contracting embryoid bodies (**B**) or by assessing the size of α-actinin-positive cell areas (**C**, **D**). Note that VAS2870 failed to reverse the antiangiogenic effect of thalidomide, whereas stimulation of cardiomyogenesis was significantly inhibited in the presence of NADPH oxidase antagonist. The free radical scavenger *N*-(2-mercaptopropionyl)glycine significantly inhibited the increase in cardiac areas observed after thalidomide administration. $^{*,\#}p < 0.05$, significantly different as indicated.

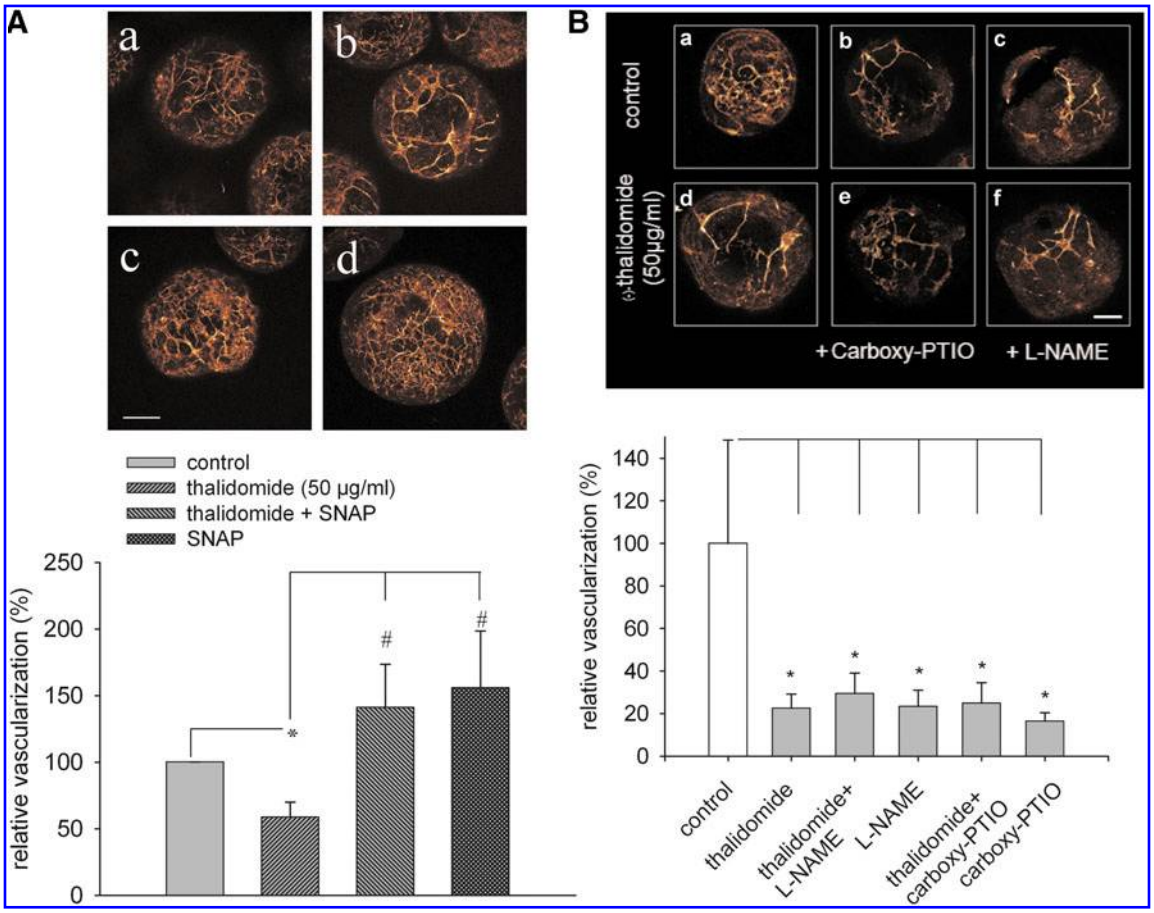
A
a
b
c
d
control
thalidomide (50 µg/ml)
thalidomide + SNAP
SNAP
relative vascularization (%)
250
200
150
100
50
0
#
#
*
B
control
(-)-thalidomide (50µg/ml)
+Carboxy-PTIO
+ L-NAME
relative vascularization (%)
140
120
100
80
60
40
20
0
control
thalidomide
thalidomide+ L-NAME
L-NAME
thalidomide+ carboxy-PTIO
carboxy-PTIO

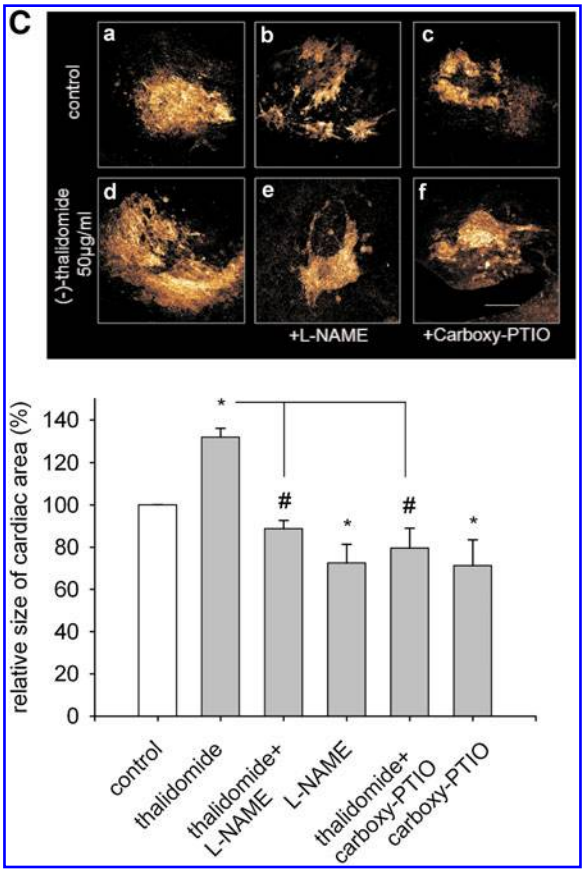
C
control
(-)-thalidomide 50µg/ml
+L-NAME
+Carboxy-PTIO
relative size of cardiac area (%)
140
120
100
80
60
40
20
0
control
thalidomide
thalidomide+ L-NAME
L-NAME
thalidomide+ carboxy-PTIO
carboxy-PTIO

activated ROS generation both *via* stimulation of NADPH oxidase and *via* the respiratory chain. However, in contrast to NADPH oxidase, ROS generation during oxidative phosphorylation apparently did not contribute to endogenous ROS production of differentiating ES cells.

Inhibition of eNOS and NO generation by thalidomide

Angiogenesis is known to be stimulated by NO generation through eNOS (38). Therefore, the antiangiogenic effects of thalidomide may be due to a decrease in NO generation and inhibition of eNOS by this compound. To address this issue, 4-day-old embryoid bodies were incubated with thalidomide in concentrations ranging from 25 to 100 μg/ml and NO generation was investigated after either 4 h (Fig. 6A, $n = 4$) or 24 h (data not shown) using the NO-sensitive fluorescence indicator DAF-FM diacetate. It was shown that thalidomide dose-dependently decreased NO generation. Incubation with the NO donor SNAP (250 n*M*) significantly increased NO levels above the untreated control following either 4 or 24 h (data not shown) of treatment. SNAP-mediated NO release abolished the effects of thalidomide (50 μg/ml) associated with inhibition of NO generation, supporting the assumption of thalidomide as an NO-modulating agent (Fig. 6B, $n = 6$). The decrease in NO generation by thalidomide could be reversed upon coadministration of the NADPH oxidase inhibitor VAS2870, which, when applied alone, increased intracellular NO levels above the untreated control. Further, the decrease in NO generation was abolished in the presence of rotenone (10 μM). Rotenone alone did not exert significant effects on basal NO levels (Fig. 6C, $n = 3$). To investigate whether the effects of thalidomide on NO generation were due to deactivation of eNOS, the phoshorylation/activation state of eNOS in the presence of 50 μg/ml thalidomide was investigated in Western blot experiments (Fig. 7, $n = 3$). It was evident that thalidomide significantly decreased eNOS phosphorylation at 5 min after incubation with the compound, whereas the expression level of nonphosphorylated eNOS remained unchanged. Significant decrease in eNOS phosphorylation when compared with the untreated control and the positive control, that is, after stimulation of eNOS with 10 μM ATP, was achieved for at least 240 min after treatment with thalidomide.

Impact of thalidomide-induced ROS and NO generation for cardiovascular differentiation of ES cells

The data of the present study demonstrate that thalidomide increases ROS and inhibits NO generation. As thalidomide stimulated cardiomyogenesis but inhibited vasculogenesis, we investigated the impact of ROS *versus* NO for cardiovascular differentiation of ES cells. To achieve this aim, 4-day-old embryoid bodies were incubated from day 4 to 10 with thalidomide (50 μg/ml) alone, with thalidomide in the presence of the NADPH oxidase inhibitor VAS2870 (50 μM), or with VAS2870 alone. As expected, thalidomide treatment decreased vascularization of embryoid bodies (Fig. 8A, $n = 3$). Notably, this effect could not be reversed upon coadministration of VAS2870, which inhibited vasculogenesis when administered alone. This indicates that low levels of NADPH oxidase-derived ROS are necessary for proper vasculogenesis of ES cells, whereas high concentrations of ROS induced by thalidomide contribute to the antiangiogenic effects exerted by this compound. In contrast to vasculogenesis, the stimulation of cardiomyogenesis achieved upon treatment of embryoid bodies with thalidomide was completely abolished in the presence of VAS2870. VAS2870 also depressed cardiomyogenesis when applied in the absence of thalidomide (Fig. 8B, C, $n = 3$). Further, coadministration of thalidomide with the free radical scavenger NMPG (100 μM) significantly reduced the increase in cardiac cell areas observed by thalidomide treatment (Fig. 8D, $n = 3$) and decreased the percentage of spontaneously contracting embryoid bodies (data not shown). The impact of NO for cardiovascular differentiation was assessed by incubating embryoid bodies either with thalidomide in combination with SNAP (250 n*M*) or with SNAP alone and assessing capillary areas by CD31 immunohistochemistry (Fig. 9A, $n = 3$). It was observed that the inhibition of vasculogenesis by thalidomide could be totally reversed upon coadministration of SNAP. Incubation with SNAP alone significantly stimulated vasculogenesis when compared with the untreated control. Likewise, treatment of embryoid bodies with SNAP increased cardiomyogenesis ($n = 3$), which, however, did not reach statistical significance (data not shown). Finally, cardiovascular differentiation was assessed following inhibition of NO generation by culturing embryoid bodies in either the presence or absence of the NOS

FIG. 9. Effects of modulation of NO on cardiovascular differentiation of ES cells. (**A**) Reversal of the antiangiogenic effects of thalidomide upon coadministration with the NO donor SNAP. Four-day-old embryoid bodies were incubated with thalidomide (50 μg/ml), with a combination of thalidomide and SNAP (250 n*M*), with SNAP alone, or remained untreated (control). Branching points in CD31-immunostained embryoid bodies were assessed by computer-assisted image analysis. *Upper panel:* Representative embryoid bodies stained with an anti-CD31 antibody are shown. (**a**) Control; (**b**) thalidomide; (**c**) thalidomide + SNAP; (**d**) SNAP. The bar represents 100 μm. *Lower panel:* Semiquantitative analysis of vascularization by computer-assisted determination of branching points. Note that the antiangiogenic effect of thalidomide was completely abolished in the presence of NO donor, which even stimulated vasculogenesis above the level of the untreated control. (**B**) Inhibition of vasculogenesis by thalidomide (50 μg/ml), applied in either the absence or presence of L-NAME (100 μM) and carboxy-PTIO. *Upper panel:* Representative embryoid bodies stained with an anti-CD31 antibody are shown. (**a**) Control; (**b**) carboxy-PTIO; (**c**) L-NAME; (**d**) thalidomide; (**e**) thalidomide + carboxy-PTIO; (**f**) thalidomide + L-NAME. The bar represents 100 μm. *Lower panel:* Semiquantitative analysis of branching points. Note that inhibition of NO generation already inhibited vasculogenesis in the absence of thalidomide treatment. (**C**) Effects of NO inhibition on the stimulation of cardiomyogenesis by thalidomide. *Upper panel:* Representative cardiac areas in embryoid bodies immunostained against α-actinin. (**a**) Control; (**b**) L-NAME; (**c**) carboxy-PTIO; (**d**) thalidomide; (**e**) thalidomide + L-NAME; (**f**) thalidomide + carboxy-PTIO. The bar represents 100 μm. *Lower panel:* Semiquantitative analysis of cardiac areas. $^{*,\#}p < 0.05$, significantly different as indicated. Carboxy-PTIO, 2-(4-carboxyphenyl)-4,4,5,5-tetramethylimidazoline-1-oxyl-3-oxide. (For interpretation of the references to color in this figure legend, the reader is referred to the web version of this article at www.liebertonline.com/ars).

inhibitor L-NAME (100 μM) or the NO scavenger carboxy-PTIO (100 μM). Under these experimental conditions, vascular differentiation was significantly impaired (Fig. 9B, $n = 3$). Notably, the increase in cardiac areas upon treatment with thalidomide was abolished in the presence of L-NAME and carboxy-PTIO. When applied alone the compounds significantly reduced the size of cardiac areas below the level of the untreated controls but did not totally abolish cardiac cell differentiation (Fig. 9C, $n = 3$).

Discussion

Thalidomide and its derivatives exert multiple effects on biological functions of cells and organs, which include activation of the immune system, antiangiogenic effects, and inhibition of cytokines (45). Previously we and others have demonstrated that the antiangiogenic effects of thalidomide may be the cause of its teratogenicity. Teratogenicity of thalidomide led to its ban from the market in the early 1960s (6, 35, 45). Notably, the antiangiogic effects of thalidomide may underlie its proven efficacy in growth inhibition of several cancers including prostate cancer, breast cancer, Karposi's sarcoma, renal cell cancer, melanoma, hepatocellular carcinoma, lung cancer, and gliomas (24). The mechanism by which thalidomide inhibits vascular growth is so far not sufficiently investigated. Thalidomide has been shown to inhibit both VEGF and basic FGF expression and secretion from tumor- (26, 46) and bone marrow stromal cells (12), and VEGF secretion, cell migration, adhesion, as well as capillary formation of human endothelial cells (22). Further, thalidomide inhibits basic FGF-induced angiogenesis *in vivo* as evaluated by the rabbit cornea micropocket assay (18). In previous studies, we as well as others have demonstrated that thalidomide and thalidomide analogs raise intracellular ROS generation (1, 10, 44), which may result in DNA damage within the embryo (33). Thalidomide elevated specifically the concentrations of highly reactive hydroxyl radicals because vasculogenesis could be restored upon coadministration of hydroxyl radical scavengers (35). It was hypothesized that the teratogenicity of thalidomide may be associated to the intracellular glutathione level in different species because it was observed that mouse embryonic fibroblasts, which are resistant to thalidomide-induced apoptosis, have higher glutathione levels than those of sensitive species (21). Further, thalidomide-induced ROS generation was six times higher in limb bud cell cultures of rabbit when compared with rat origin, which was attributed to a different glutathione depletion in the nuclear *versus* cytoplasmic compartment by thalidomide in the different species (14). In the present study, we investigated the effects of thalidomide on vasculogenesis of ES cells in more detail. We found that thalidomide in concentration-dependent manner downregulated vascular sprout formation in differentiating embryoid bodies. Further, thalidomide strongly inhibited the vascularization of multicellular tumor spheroids in confrontation cultures, which were previously established by us as a novel *in vitro* system to study tumor angiogenesis (48). Interestingly, thalidomide did not decrease the cell numbers of CD31- and CD144-positive cells, suggesting that this compound did not interfere with vascular progenitor cell differentiation, but with vascular sprouting and tube formation. This observation is supported by recent data demonstrating that the thalidomide analog lenalidomide consistently inhibited both sprout formation by arterial rings and cord formation by endothelial cells in a dose-dependent manner (27). Notably, the inhibition of vasculogenesis by thalidomide in embryoid bodies was paralleled by an enhancement of cardiomyogenesis. This observation is of importance because it has been previously demonstrated that cardiac and vascular cells are differentiating from a common precursor (17). Further, the teratogenic effects of thalidomide in humans and laboratory animals are associated with heart malformations including ventricular septal defects, right atrial distension primarily involving the coronary sinus, malpositioned great vessels, and narrowed left ventricular chamber with hypertrophied walls (19, 39, 40).

The enhancement of cardiomyogenesis of differentiating ES cells may be due to the increased generation of ROS by this compound. This notion sounds reasonable because we have previously demonstrated that exogenous addition of ROS (5) as well as physical ROS-generating maneuvers on ES cells, for example, mechanical strain (37) or electromagnetic fields (36) to differentiating ES cells, stimulated cardiac cell differentiation. Notably, in the present study, treatment with free radical scavenger NMPG inhibited the effect of thalidomide on cardiac cell differentiation. To address the role of ROS on the impairment of cardiovascular differentiation of ES cells, the sources of ROS generation were investigated using pharmacological inhibitors of NADPH oxidase (VAS2870) and the mitochondrial respiratory chain complex I inhibitor rotenone. It was apparent that upon inhibition of NADPH oxidase the thalidomide-induced increase in ROS was totally abolished. Additionally, VAS2870, when applied alone, significantly depressed ROS generation below the level of the untreated control. This suggests that ROS generation *via* NADPH oxidase is the primordial mechanism under physiological conditions and may be overactivated by thalidomide. An increase in NOX-1, NOX-2, and NOX-4 expression by thalidomide was excluded in our experiments. Inhibition of the respiratory chain only abolished the increase in ROS generation by thalidomide, whereas rotenone alone did not impair ROS generation under control conditions. These observations point toward the direction that, in addition to activation of NADPH oxidase, thalidomide may interfere with oxidative phosphorylation and mitochondrial function. In this respect, it has been recently shown that the thalidomide analog CPS49 disrupted mitochondrial integrity and elevated ROS in human leukemic cells (9). The impact of specific NOX isoforms for thalidomide-induced cardiomyogenesis was assessed by generation of shRNA gene-inactivated NOX-1 and NOX-4 cell lines. NOX-1 as well as NOX-4 gene-inactivated ES cells were significantly impaired in their capacity for cardiomyogenic differentiation. Further, thalidomide failed to stimulate cardiomyogenesis, whereas a partial rescue could be achieved by exogenous addition of H_2O_2, which significantly stimulated cardiomyogenesis when applied in the absence of thalidomide.

Besides oxygen intermediates, NO is also a decisive signaling molecule regulating cardiovascular differentiation processes in ES cells. Above all, endothelial cell differentiation in ES cells is dependent on NO generation (16). We therefore hypothesized that thalidomide while elevating ROS may depress NO generation, thereby inhibiting vasculogenesis of ES cells. In endothelial cells, it has been recently shown that thalidomide attenuates NO-driven angiogenesis by inhibiting cell migration (42) and interacting with soluble

guanylyl cyclase (28). Indeed, our data demonstrated that thalidomide treatment decreased NO generation in differentiating embryoid bodies within 4 h. Interestingly, the inhibition of NO generation by thalidomide could be reversed by coadministration of VAS2870. However, VAS2870, when applied alone, significantly increased NO generation above the level of the untreated control. This observation is of importance because VAS2870 in the presence of thalidomide did not rescue vasculogenesis, and VAS2870 alone significantly inhibited vascular sprout formation. The decrease in NO generation by thalidomide was presumably due to dephosphorylation of eNOS, which occurred within few minutes. The mechanism by which thalidomide is inhibiting eNOS is so far not known. However, recent data have shown that in contrast to short-time application of ROS, which stimulates eNOS activity, long-time and repetitive application of ROS to endothelial cells decreased eNOS activity and NO generation (4). Further, H_2O_2 treatment of ovine pulmonary arterial endothelial cells has been demonstrated to decrease eNOS promoter activity by inhibition of SP-1 activity (23). Another explanation for the reduction in eNOS activity and NO generation by thalidomide may be related to the decrease in VEGF expression and secretion by this compound (22). VEGF is well known to activate eNOS and to stimulate NO and peroxynitrite production, thereby initiating endothelial cell migration and tube formation (7, 8). If indeed the decrease in NO generation due to thalidomide treatment of embryoid bodies is responsible for the antiangiogenic effect of this compound, it may be assumed that the effect is abolished if NO generation is increased. This assumption was corroborated by experiments where NO generation was elevated by the NO donor SNAP. This treatment totally abolished the antiangiogenic effects of thalidomide and increased vasculogenesis above the level of the untreated control, thus underscoring the impact of NO for vascular differentiation of ES cells.

Thalidomide and its analogs are currently evaluated in several life-threatening diseases as promising remedies. To avoid the teratogenic side effects of these compounds and to understand their beneficial effects in antiangiogenic therapy, it is inevitably necessary to unravel their mechanisms of action. The data of the present study clearly demonstrate that, in ES cells, thalidomide changes the balance of vasculogenesis to cardiomyogenesis in differentiating ES cells. The procardiomyogenic effects of thalidomide are apparently due to stimulation of ROS generation, whereas the adverse effects on endothelial cell sprouting, vascular tube formation, and tumor vascularization are due to downregulation of NO generation. NO donors are still discussed as potential anticancer therapeutics even in the treatment of multiple myeloma (20) and are used in the treatment of cardiovascular diseases (41). Their coadministration with thalidomide should therefore be handled with care because systemic elevation of NO may counteract the antiangiogenic activity of this promising and widely applicable drug, thereby declining its beneficial action.

Acknowledgments

This work was supported by the SET Foundation for the replacement of animal experimentation (Frankfurt, Germany), by the Excellence Cluster Cardiopulmonary System (ECCPS), and by a research grant from the University Medical Center Gießen and Marburg (UKGM).

Author Disclose Statement

No competing financial interests exist.

References

1. Aerbajinai W, Zhu J, Gao Z, Chin K, and Rodgers GP. Thalidomide induces gamma-globin gene expression through increased reactive oxygen species-mediated p38 MAPK signaling and histone H4 acetylation in adult erythropoiesis. *Blood* 110: 2864–2871, 2007.
2. Aragon-Ching JB, Li H, Gardner ER, and Figg WD. Thalidomide analogues as anticancer drugs. *Recent Pat Anticancer Drug Discov* 2: 167–174, 2007.
3. Bekhite MM, Finkensieper A, Abou-Zaid FA, El Shourbagy IK, Omar KM, Figulla HR, Sauer H, and Wartenberg M. Static electromagnetic fields induce vasculogenesis and chondro-osteogenesis of mouse embryonic stem cells by reactive oxygen species-mediated upregulation of vascular endothelial growth factor. *Stem Cells Dev* 19: 731–743, 2010.
4. Boulden BM, Widder JD, Allen JC, Smith DA, Al Baldawi RN, Harrison DG, Dikalov SI, Jo H, and Dudley SC, Jr. Early determinants of H2O2-induced endothelial dysfunction. *Free Radic Biol Med* 41: 810–817, 2006.
5. Buggisch M, Ateghang B, Ruhe C, Strobel C, Lange S, Wartenberg M, and Sauer H. Stimulation of ES-cell-derived cardiomyogenesis and neonatal cardiac cell proliferation by reactive oxygen species and NADPH oxidase. *J Cell Sci* 120: 885–894, 2007.
6. D'Amato RJ, Loughnan MS, Flynn E, and Folkman J. Thalidomide is an inhibitor of angiogenesis. *Proc Natl Acad Sci USA* 91: 4082–4085, 1994.
7. Dimmeler S, Dernbach E, and Zeiher AM. Phosphorylation of the endothelial nitric oxide synthase at ser-1177 is required for VEGF-induced endothelial cell migration. *FEBS Lett* 477: 258–262, 2000.
8. El Remessy AB, Al Shabrawey M, Platt DH, Bartoli M, Behzadian MA, Ghaly N, Tsai N, Motamed K, and Caldwell RB. Peroxynitrite mediates VEGF's angiogenic signal and function via a nitration-independent mechanism in endothelial cells. *FASEB J* 21: 2528–2539, 2007.
9. Ge Y, Byun JS, De Luca P, Gueron G, Yabe IM, Sadiq-Ali SG, Figg WD, Quintero J, Haggerty CM, Li QQ, De Siervi A, and Gardner K. Combinatorial antileukemic disruption of oxidative homeostasis and mitochondrial stability by the redox reactive thalidomide 2-(2,4-difluoro-phenyl)-4,5,6,7-tetrafluoro-1H-isoindole-1,3(2H)-dione (CPS49) and flavopiridol. *Mol Pharmacol* 74: 872–883, 2008.
10. Ge Y, Montano I, Rustici G, Freebern WJ, Haggerty CM, Cui W, Ponciano-Jackson D, Chandramouli GV, Gardner ER, Figg WD, Abu-Asab M, Tsokos M, Jackson SH, and Gardner K. Selective leukemic-cell killing by a novel functional class of thalidomide analogs. *Blood* 108: 4126–4135, 2006.
11. Gunther S, Ruhe C, Derikito MG, Bose G, Sauer H, and Wartenberg M. Polyphenols prevent cell shedding from mouse mammary cancer spheroids and inhibit cancer cell invasion in confrontation cultures derived from embryonic stem cells. *Cancer Lett* 250: 25–35, 2007.
12. Gupta D, Treon SP, Shima Y, Hideshima T, Podar K, Tai YT, Lin B, Lentzsch S, Davies FE, Chauhan D, Schlossman RL, Richardson P, Ralph P, Wu L, Payvandi F, Muller G, Stirling

DI, and Anderson KC. Adherence of multiple myeloma cells to bone marrow stromal cells upregulates vascular endothelial growth factor secretion: therapeutic applications. *Leukemia* 15: 1950–1961, 2001.
13. Hansen JM and Harris C. A novel hypothesis for thalidomide-induced limb teratogenesis: redox misregulation of the NF-kappaB pathway. *Antioxid Redox Signal* 6: 1–14, 2004.
14. Hansen JM, Harris KK, Philbert MA, and Harris C. Thalidomide modulates nuclear redox status and preferentially depletes glutathione in rabbit limb versus rat limb. *J Pharmacol Exp Ther* 300: 768–776, 2002.
15. Hicks LK, Haynes AE, Reece DE, Walker IR, Herst JA, Meyer RM, and Imrie K. A meta-analysis and systematic review of thalidomide for patients with previously untreated multiple myeloma. *Cancer Treat Rev* 34: 442–452, 2008.
16. Huang N, Fleissner F, Sun J, and Cooke J. Role of nitric oxide signaling in endothelial differentiation of embryonic stem cells. *Stem Cells Dev* 2010 [Epub ahead of print].
17. Kattman SJ, Huber TL, and Keller GM. Multipotent flk-1+ cardiovascular progenitor cells give rise to the cardiomyocyte, endothelial, and vascular smooth muscle lineages. *Dev Cell* 11: 723–732, 2006.
18. Kenyon BM, Browne F, and D'Amato RJ. Effects of thalidomide and related metabolites in a mouse corneal model of neovascularization. *Exp Eye Res* 64: 971–978, 1997.
19. Khera KS. Fetal cardiovascular and other defects induced by thalidomide in cats. *Teratology* 11: 65–69, 1975.
20. Kiziltepe T, Hideshima T, Ishitsuka K, Ocio EM, Raje N, Catley L, Li CQ, Trudel LJ, Yasui H, Vallet S, Kutok JL, Chauhan D, Mitsiades CS, Saavedra JE, Wogan GN, Keefer LK, Shami PJ, and Anderson KC. JS-K, a GST-activated nitric oxide generator, induces DNA double-strand breaks, activates DNA damage response pathways, and induces apoptosis *in vitro* and *in vivo* in human multiple myeloma cells. *Blood* 110: 709–718, 2007.
21. Knobloch J, Reimann K, Klotz LO, and Ruther U. Thalidomide resistance is based on the capacity of the glutathione-dependent antioxidant defense. *Mol Pharm* 5: 1138–1144, 2008.
22. Komorowski J, Jerczynska H, Siejka A, Baranska P, Lawnicka H, Pawlowska Z, and Stepien H. Effect of thalidomide affecting VEGF secretion, cell migration, adhesion and capillary tube formation of human endothelial EA.hy 926 cells. *Life Sci* 78: 2558–2563, 2006.
23. Kumar S, Sun X, Wiseman DA, Tian J, Umapathy NS, Verin AD, and Black SM. Hydrogen peroxide decreases endothelial nitric oxide synthase promoter activity through the inhibition of Sp1 activity. *DNA Cell Biol* 28: 119–129, 2009.
24. Kumar S, Witzig TE, and Rajkumar SV. Thalidomid: current role in the treatment of non-plasma cell malignancies. *J Clin Oncol* 22: 2477–2488, 2004.
25. Lenz W. Thalidomide and congenital abnormalitie. *J Am Med Assoc* 1: 45, 1962.
26. Li X, Liu X, Wang J, Wang Z, Jiang W, Reed E, Zhang Y, Liu Y, and Li QQ. Thalidomide down-regulates the expression of VEGF and bFGF in cisplatin-resistant human lung carcinoma cells. *Anticancer Res* 23: 2481–2487, 2003.
27. Lu L, Payvandi F, Wu L, Zhang LH, Hariri RJ, Man HW, Chen RS, Muller GW, Hughes CC, Stirling DI, Schafer PH, and Bartlett JB. The anti-cancer drug lenalidomide inhibits angiogenesis and metastasis via multiple inhibitory effects on endothelial cell function in normoxic and hypoxic conditions. *Microvasc Res* 77: 78–86, 2009.
28. Majumder S, Rajaram M, Muley A, Reddy HS, Tamilarasan KP, Kolluru GK, Sinha S, Siamwala JH, Gupta R, Ilavarasan R, Venkataraman S, Sivakumar KC, Anishetty S, Kumar PG, and Chatterjee S. Thalidomide attenuates nitric oxide-driven angiogenesis by interacting with soluble guanylyl cyclase. *Br J Pharmacol* 158: 1720–1734, 2009.
29. McBride WG. Thalidomide and congenital abnormalities. *J Am Med Assoc* 2: 1358, 1961.
30. Mei SC and Wu RT. The G-rich promoter and G-rich coding sequence of basic fibroblast growth factor are the targets of thalidomide in glioma. *Mol Cancer Ther* 7: 2405–2414, 2008.
31. Melchert M and List A. The thalidomide saga. *Int J Biochem Cell Biol* 39: 1489–1499, 2007.
32. Paravar T and Lee DJ. Thalidomide: mechanisms of action. *Int Rev Immunol* 27: 111–135, 2008.
33. Parman T, Wiley MJ, and Wells PG. Free radical-mediated oxidative DNA damage in the mechanism of thalidomide teratogenicity. *Nat Med* 5: 582–585, 1999.
34. Sauer H, Bekhite MM, Hescheler J, and Wartenberg M. Redox control of angiogenic factors and CD31-positive vessel-like structures in mouse embryonic stem cells after direct current electrical field stimulation. *Exp Cell Res* 304: 380–390, 2005.
35. Sauer H, Gunther J, Hescheler J, and Wartenberg M. Thalidomide inhibits angiogenesis in embryoid bodies by the generation of hydroxyl radicals. *Am J Pathol* 156: 151–158, 2000.
36. Sauer H, Rahimi G, Hescheler J, and Wartenberg M. Effects of electrical fields on cardiomyocyte differentiation of embryonic stem cells. *J Cell Biochem* 75: 710–723, 1999.
37. Schmelter M, Ateghang B, Helmig S, Wartenberg M, and Sauer H. Embryonic stem cells utilize reactive oxygen species as transducers of mechanical strain-induced cardiovascular differentiation. *FASEB J* 20: 1182–1184, 2006.
38. Sessa WC. Molecular control of blood flow and angiogenesis: role of nitric oxide. *J Thromb Haemost* 7 Suppl 1: 35–37, 2009.
39. Smithells RW. Defects and disabilities of thalidomide children. *Br Med J* 1: 269–272, 1973.
40. Smithells RW and Newman CG. Recognition of thalidomide defects. *J Med Genet* 29: 716–723, 1992.
41. Strijdom H, Chamane N, and Lochner A. Nitric oxide in the cardiovascular system: a simple molecule with complex actions. *Cardiovasc J Afr* 20: 303–310, 2009.
42. Tamilarasan KP, Kolluru GK, Rajaram M, Indhumathy M, Saranya R, and Chatterjee S. Thalidomide attenuates nitric oxide mediated angiogenesis by blocking migration of endothelial cells. *BMC Cell Biol* 7: 17, 2006.
43. Teo SK. Properties of thalidomide and its analogues: implications for anticancer therapy. *AAPS J* 7: E14–E19, 2005.
44. Thadani NA, McNamee JP, and Winn LM. Thalidomide alters c-MYB and PIM-1 signaling in K-562 cells. *Pharmacol Res* 54: 91–96, 2006.
45. Therapontos C, Erskine L, Gardner ER, Figg WD, and Vargesson N. Thalidomide induces limb defects by preventing angiogenic outgrowth during early limb formation. *Proc Natl Acad Sci USA* 106: 8573–8578, 2009.
46. Trussardi-Regnier A, Lavenus S, Gorisse MC, and Dufer J. Thalidomide alters nuclear architecture without ABCB1 gene modulation in drug-resistant myeloma cells. *Int J Oncol* 35: 641–647, 2009.
47. Walker SL, Waters MF, and Lockwood DN. The role of thalidomide in the management of erythema nodosum leprosum. *Lepr Rev* 78: 197–215, 2007.
48. Wartenberg M, Donmez F, Ling FC, Acker H, Hescheler J, and Sauer H. Tumor-induced angiogenesis studied in confrontation cultures of multicellular tumor spheroids and

embryoid bodies grown from pluripotent embryonic stem cells. *FASEB J* 15: 995–1005, 2001.

49. Yagyu T, Kobayashi H, Matsuzaki H, Wakahara K, Kondo T, Kurita N, Sekino H, Inagaki K, Suzuki M, Kanayama N, and Terao T. Thalidomide inhibits tumor necrosis factor-alpha-induced interleukin-8 expression in endometriotic stromal cells, possibly through suppression of nuclear factor-kappaB activation. *J Clin Endocrinol Metab* 90: 3017–3021, 2005.

Address correspondence to:
Dr. Heinrich Sauer
Department of Physiology
Justus Liebig University Giessen
Aulweg 129
35392 Giessen
Germany

E-mail: heinrich.sauer@physiologie.med.uni-giessen.de

Date of first submission to ARS Central, February 4, 2010; date of final revised submission, May 6, 2010; date of acceptance, June 2, 2010.

Abbreviations Used

Carboxy-PTIO = 2-(4-carboxyphenyl)-4,4,5,5-tetramethylimidazoline-1-oxyl-3-oxide
DAF = triazolofluorescein
DAF-FM = 4-amino-5-methylamino-2′,7′-difluorofluorescein
DCF = 2′,7′-dichlorofluorescein
EDTA = ethylenediaminetetraacetic acid
eNOS = endothelial NO synthase
ES = embryonic stem
FCS = fetal calf serum
FGF-2 = fibroblast growth factor-2
H_2DCF-DA = 2′,7′-dichlorodihydrofluorescein diacetate
L-NAME = N^G-nitro-L-arginine methyl ester
NMPG = *N*-(2-mercaptopropionyl)glycine
NO = nitric oxide
PBS = phosphate-buffered saline
PBST = PBS containing 0.01% Triton X-100
ROS = reactive oxygen species
SNAP = *S*-nitrosopenicillamine
VEGF = vascular endothelial growth factor

This article has been cited by:

1. Eugenia Cifuentes-Pagano, Gabor Csanyi, Patrick J. Pagano. 2012. NADPH oxidase inhibitors: a decade of discovery from Nox2ds to HTS. *Cellular and Molecular Life Sciences* **69**:14, 2315-2325. [CrossRef]